Mode Description of Routes to Chaos in External-Cavity Coupled Semiconductor Lasers

Yao Huang Kao, *Member,* Nien Ming Wang, and Hong Ming Chen

Abstract—**The nonlinear behaviors of routes to chaos in semiconductor lasers with external optical feedback were explored in this work. It was indicated that the relaxation oscillation was the origin of the first nonlinear instability of optical intensity under a short delay. Three types of transition routes with quasi-periodic, subharmonic oscillation, and periodic doubling to optical chaos were distinguished in terms of the delay time normalized to the inverse of the relaxation oscillation frequency of a solitary laser diode. The linearized mode theory and small-signal response were confirmed as part of the phenomena in the transitions to chaos.**

I. Introduction

THE optical feedback in semiconductor lasers has received a substantial amount of attention owing to its practical importance as well as to the wide variety of nonlinear properties. This effect has often been employed for reducing the optical linewidth so as to satisfy the requirements for some applications, such as coherent communication and interferometric fiber sensors. In these applications, the feedback strength is operated either at low feedback (< -40 dB) [1], [2] or at strong feedback with an antireflective coating on the laser facet [3]. Within the considerable region of medium feedback levels, the linewidth is observed to become broadened to several gigahertz and is confirmed to be closely related to the coherence collapse, in which the optical intensity fluctuates in a complicated way [4]–[18]. The infinitely dimensional nature of the delay system is actually capable of giving rise to an extensive variety of nonlinear behaviors. Several types of chaotic transitions have been observed experimentally in some specific situations. The most noticeable behavior is quasi-periodic route (QP), in which the relaxation oscillation and external-cavity frequencies occur sequentially and are incommensurate with external-cavity length, of a few tens of centimeters [10], [12], [14]. The intermittent behaviors with the relaxation pulse modulated by the external cavity frequency have been found in a situation with the bias current around the kink region in the L–I curve and with feedback from the medium to strong feedback regime [15], [16]. Subharmonic cascaded bifurcations have also been observed with a relatively strong feedback level [5], [7], [18].

The cavity formed by external feedback takes actions not only in the optical frequency but also in the microwave range, which is subject to an optical intensity fluctuation. Hence, the coupled-cavity laser contains a number of resonant frequencies for the intensity fluctuations, i.e., the temporal relaxation oscillation frequency due to the electro–optical interaction and a series of spatial external-cavity frequencies. The competition and interplay between these natural frequencies arise as the feedback level is increased. A successive occurrence of instabilities provide the chaotic fluctuation in the optical intensity. The theoretical study of feedback effects on the intensity instability are usually based on the rate equations [19], which have been proven to contain the dominant information observed experimentally [10], [12]–[14], [16]–[18]. Simulations of a nonlinear injection-locking model have indicated a periodic-doubling cascade (PD) under decreasing feedback levels in a long external cavity [11]. The numerical results for the coherence collapse in a short external cavity have been presented, but without dealing with the transitions to chaos [20], [21]. Indeed, the periodic-doubling phenomena have been presented, however, with parameters deep in the complicated region [11], [18]. It is still interesting to extract the situation for the respective routes, especially for the periodic-doubling route at the actual beginning of the feedback level. The purpose of this paper is to investigate the dynamic transitions with an external cavity length of about 2–11 cm, which is equivalent to having the fundamental frequency of the cavity modes vary from twice to half that of the relaxation oscillation frequency, in order to test the periodic-doubling route. For convenience, the delay ratio τf_{rsol}, which is defined by the external delay time τ normalized to the inverse of the relaxation oscillation frequency f_{rsol} of the solitary laser, is employed so as to distinguish the feedback distance in the study. The first instabilities are forecasted in connection with the linearized mode theory. These investigations are not only of fundamental interest but also are the foundation of some

Manuscript received May 31, 1993; revised January 4, 1994. This work was supported by the National Science Council, Republic of China, under Contract NSC 82-0417-E-009-133.

Y. H. Kao and N. M. Wang are with the Institute of Communication Engineering and Center of Telecommunication Research, National Chiao-Tung University, Hsinchu, Taiwan 30050, Republic of China.

H. M. Chen is with the Opto-Electronics and System Laboratory, Industrial Technology Research Institute, Hsinchu, Taiwan 30050, Republic of China.

IEEE Log Number 9402329.

applications for the practical employment of optical devices, e.g., short pulse generations [22]–[24].

The organization of the paper is as follows. The rate equations in terms of photon density, carrier density, and optical phase are described in Section II. The nonlinear instabilities from the small-signal approach are also presented. Of special focus is the origin of the first instabilities. Section III summarizes the numerical results of transitions to chaos under the various delay ratios. Three types of routes to chaos, i.e., the quasi-periodic route, the subharmonic-oscillation route, and the periodic-doubling route are distinguished from each other. The onset frequency and threshold feedback level of the first oscillation are also put into comparison with those predicted from the small-signal approach. The concluding remarks are given in Section IV.

II. Rate Equations and Small-Signal Approach

In the study, the feedback is assumed to come from a flat mirror with a reflectivity of R_3. R_1 and R_2 are the reflectivities of the laser facets. According to the previous work [19], the complex electric field $E(t)$ of the outgoing field, which is situated at the internal laser facet opposite to the external cavity, satisfies the commonly used equation

$$\frac{d}{dt}E(t) = \left\{ j\omega(n) + \frac{1}{2}\left[G(n, E_0^2) - \frac{1}{\tau_p} \right] \right\} E(t) + k_c E(t - \tau) \quad (1)$$

where $G(n, E_0^2)$ is the optical gain and is dependent of optical intensity E_0^2, $n(t)$ is the carrier density in the active region, τ_p is the photon lifetime, τ is the round-trip delay of the external cavity, and $\omega(n)$ is the carrier-dependent optical angular frequency under single-longitudinal-mode operation. To account for the gain saturation, the gain $G(n, E_0^2)$ and angular frequency $\omega(n)$ are assumed to be $G(n, E_0^2) = g(n - n_0)(1 - \epsilon E_0^2)$, and $\omega(n) = \omega_0 + \alpha g(n - n_{\text{th}})/2$, respectively, where ω_0 is the optical angular frequency without optical feedback, g is the differential gain coefficient, n_0 is the carrier density for transparency, ϵ is the gain saturation factor, α is the linewidth enhancement factor, and n_{th} is the threshold carrier density of the solitary laser. The term $k_c E(t - \tau)$ accounts for external reflection and renders the system of (1) infinitely dimensional. Under the assumption of a single reflection, the feedback coefficient k_c is expressed as [25]

$$k_c = \frac{1}{\tau_d} \frac{1 - R_2}{\sqrt{R_2}} \sqrt{R_{\text{ext}}} \quad (2)$$

where τ_d is the internal round-trip delay of laser cavity and R_{ext} is the ratio of the reflected power entering the laser at the laser facet to the emitted power per facet. The ratio R_{ext} can be related to R_3 via $R_{\text{ext}} = R_3 \eta_c^2 e^{-2\alpha_f L_{\text{ext}}}$, where η_c is the power-coupling efficiency, α_f is the absorption coefficient, and L_{ext} is the length of the external cavity [26]. The ratio R_{ext} is the controlled parameter in the study. The optical field can generally be written

$$E(t) = E_0(t) e^{j[\omega_0 t + \phi(t)]} \quad (3)$$

where the amplitude $E_0(t)$ and the phase $\phi(t)$ are assumed to be real and slowly time varying. The E field is further replaced by the measurable quantity of the photon density $S(t) = E_0^2(t)$. Substituting (3) into (1) and taking the extra effect of the spontaneous emission into account, a set of equations governing the $S(t)$ and $\phi(t)$ can then be obtained as [8]

$$\frac{d}{dt}S(t) = \left[g(n(t) - n_0)(1 - \epsilon S(t)) - \frac{1}{\tau_p} \right] S(t) + \frac{\beta n(t)}{\tau_e} + 2k_c \sqrt{S(t)S(t - \tau)} \cos[\omega_0 \tau + \phi(t) - \phi(t - \tau)] \quad (4)$$

$$\frac{d}{dt}\phi(t) = \frac{\alpha g(n(t) - n_{\text{th}})}{2} - k_c \frac{\sqrt{S(t - \tau)}}{\sqrt{S(t)}} \sin[\omega_0 \tau + \phi(t) - \phi(t - \tau)] \quad (5)$$

where β is the spontaneous emission factor. These two equations must be solved in conjunction with the rate equation for the carrier density $n(t)$

$$\frac{d}{dt}n(t) = \frac{I}{eV} - \frac{n(t)}{\tau_e} - g(n(t) - n_0)[1 - \epsilon S(t)]S(t) \quad (6)$$

where V is the active volume of the laser cavity, τ_e is the carrier lifetime, e is the electronic charge and I is the injection current. Such nonlinear equations can be solved numerically. The typical parameters, as appropriate for a long wavelength InGaAsP laser diode, are given in Table I [26], [27].

As a matter of fact, the inherent properties of a solitary laser may play an important role in considering the emergence of intensity instabilities. As subjected to the intensity fluctuation, the laser diode can be modeled as a second-order low-pass filter with the transfer function rolling off 12 dB/octave above the relaxation oscillation frequency. Three fundamental parameters of the relaxation oscillation frequency f_{rsol}, the damping factor η, and the resonance amplitude H_{max} of transfer function $H(j2\pi f)$ are of special importance in describing the response. From (4) and (6) with no feedback $k_c = 0$, the relaxation oscillation frequency f_{rsol}, the damping factor η, and the resonance amplitude H_{max} of $H(j2\pi f)$ are capable of being expressed as

$$f_{\text{rsol}} = (gS_0/\tau_p)^{1/2}/(2\pi) \quad (7)$$

$$\eta = \left[1/\tau_e + gS_t + S_t \epsilon/\tau_p + \beta I_{\text{th}}/(eVS_t) \right]/(4\pi f_{\text{rsol}}) \quad (8)$$

$$H_{\text{max}} = (gS_0/\tau_p)^{1/2} / \left[\beta I_{\text{th}}/(eVS_0) + gS_0 + \epsilon S_0/\tau_p + 1/\tau_e \right] \quad (9)$$

respectively, where S_0 is the stationary photon density without optical feedback, $I_{\text{th}} = eVn_{\text{th}}/\tau_e$, $S_t = \tau_p(I -$

TABLE I
LASER PARAMETERS

Laser Diode Parameters	
V (laser diode cavity volume)	$= 1\times10^{-16}$ m^3
τ_d (laser diode cavity round–trip delay)	= 6.67ps
τ_p (photon lifetime)	= 1.6ps
τ_e (carrier lifetime)	= 2ns
α (linewidth enhancement factor)	= 5
β (spontaneous emission factor)	$=1\times10^{-5}$
g (linear gain coefficient)	$= 1.5\times10^{-12}$ m^3/s
ϵ (gain saturation factor)	$= 1.76\times10^{-23}$ m^3
n_o (transparent carrier density)	$= 1\times10^{24}$m^{-3}
R_1, R_2 (power reflection coefficient)	= 0.32
I (bias current)	$= 1.3I_{th}$
External Cavity Parameters	
L_{ext} (external cavity length)	= 2cm to 11cm
$\omega_0\tau$ (feedback phase)	$= -\arctan(\alpha)$

$I_{th})/eV$. The typical value of the damping factor is indicated from previous literature to be around 0.1 for InGaAsP lasers. The gain saturation factor ϵ has the strongest influence on laser damping as a major result of (9). In the observed case, $\eta \cong 0.133$ and $H_{max} \simeq 3.7345$. The effect of feedback gives rise to a modification of the transfer function. An oscillation occurs at the condition of infinite gain or the denominator of the modified transfer function being equal to zero. After algebraic manipulations from (4)–(6) around a stationary state, the denominator of the modified transfer function after a Laplace transform is obtained as [28]

$$\begin{aligned} D(z) = z^3 &+ \left[C_1 + C_2 + C_3 + \frac{1}{\tau_e} + 2\kappa\cos\omega\tau\right]z^2 \\ &+ \left[C_1C_5 - C_4C_5 + \kappa^2 + (C_1 + C_2)\right. \\ &\cdot\left.\left(\kappa\cos\omega\tau + \frac{1}{\tau_e} + C_3\right) + 2\kappa\cos\omega\tau\left(\frac{1}{\tau_e} + C_3\right)\right]z \\ &+ \left[\kappa C_1C_5\cos\omega\tau - \kappa C_4\alpha gS_s\sin\omega\tau\right. \\ &- \kappa C_4C_5\cos\omega\tau + \kappa C_1\alpha gS_s\sin\omega\tau \\ &+ (C_1 + C_2)\left(\frac{1}{\tau_e} + C_3\right)\kappa\cos\omega\tau \\ &+ \left.\left(\frac{1}{\tau_e} + C_3\right)\kappa^2\right] \end{aligned} \tag{10}$$

where $\kappa = k_c(1 - e^{-z\tau})$, $C_1 = g(n_s - n_0)\epsilon S_s$, $C_2 = \beta n_s/(\tau_e S_s)$, $C_3 = g(1 - \epsilon S_s)S_s$, $C_4 = g(n_s - n_0)(1 - \epsilon S_s)$, $C_5 = -[g(1 - \epsilon S_s)S_s + \beta/\tau_e]$, n_s is the carrier density, and S_s is the photon density of the stationary state. The critical conditions for the first oscillation can be obtained as a zero of $D(z)$ is crossing the imaginary axis. This case is also referred to as a Hopf bifurcation from the bifurcation viewpoint [17]. A so-called limit-cycle solution is obtained after the Hopf bifurcation. Substituting $z = j\Omega$ and separating the real and imaginary parts in (10), we obtain two relations as

$$X_2k_c^2 + X_1k_c + X_0 = 0 \tag{11}$$

$$Y_2k_c^2 + Y_1k_c + Y_0 = 0 \tag{12}$$

where

$$\begin{aligned} X_2 &= [(1 - \cos\Omega\tau)^2 - (\sin\Omega\tau)^2]\left(\frac{1}{\tau_e} + C_3\right) \\ &\quad - 2\Omega(1 - \cos\Omega\tau)\sin\Omega\tau \\ X_1 &= (1 - \cos\Omega\tau)\left[-2\Omega^2\cos\omega\tau - C_4\alpha gS_s\sin\omega\tau\right. \\ &\quad - C_4C_5\cos\omega\tau + C_1C_5\cos\omega\tau + C_1\alpha gS_s\sin\omega\tau \\ &\quad + (C_1 + C_2)\left(\frac{1}{\tau_e} + C_3\right)\cos\omega\tau\Big] \\ &\quad - \Omega(C_1 + C_2)\sin\Omega\tau\cos\omega\tau \\ &\quad - 2\Omega\left(\frac{1}{\tau_e} + C_3\right)\sin\Omega\tau\cos\omega\tau \\ X_0 &= -\Omega^2\left(C_1 + C_2 + C_3 + \frac{1}{\tau_e}\right) \\ Y_2 &= \Omega(1 - \cos\Omega\tau)^2 - \Omega(\sin\Omega\tau)^2 \\ &\quad + 2(1 - \cos\Omega\tau)\left(\frac{1}{\tau_e} + C_3\right)\sin\Omega\tau \\ Y_1 &= \sin\Omega\tau\left[-2\Omega^2\cos\omega\tau - C_4\alpha gS_s\sin\omega\tau\right. \\ &\quad + C_1C_5\cos\omega\tau + C_1\alpha gS_s\sin\omega\tau \\ &\quad - C_4C_5\cos\omega\tau + (C_1 + C_2)\left(\frac{1}{\tau_e} + C_3\right)\cos\omega\tau\Big] \\ &\quad + \Omega(C_1 + C_2)(1 - \cos\Omega\tau)\cos\omega\tau \\ &\quad + 2\Omega(1 - \cos\Omega\tau)\left(\frac{1}{\tau_e} + C_3\right)\cos\omega\tau \end{aligned}$$

and

$$Y_0 = -\Omega^3 + \Omega(C_1C_5 - C_4C_5) + \Omega(C_1 + C_2)\left(\frac{1}{\tau_e} + C_3\right).$$

The solution of the onset angular frequency Ω and the feedback strength k_c in coupled-equations (11) and (12) can be found after some numerical procedures. For comparison, the results equal those presented in [28, eq. (41)], which are obtained simply by neglecting the quadratic terms of k_c in (11) and (12) and approximating the photon

density S_s and carrier density n_s as the unperturbed ones, are also given as

$$x = \frac{1}{y\pi}\left(\cot^{-1}\left(u\left(y - \frac{1}{y}\right)\right) + m\pi\right) \tag{13}$$

$$k_c = \frac{y^2 + u^2(y^2 - 1)^2}{2v\sqrt{\alpha^2 + (2y^2 - 1)^2}} \tag{14}$$

where $x = \tau f_{\text{rsol}}$ is the delay ratio, $y = \Omega/(2\pi f_{\text{rsol}})$ is the normalized onset oscillation frequency, $u = 2\pi f_{\text{rsol}}/(1/\tau_e + (\tau_p + \epsilon/g)4\pi^2 f_{\text{rsol}}^2)$, $v = 1/(1/\tau_e + (\tau_p + \epsilon/g)4\pi^2 f_{\text{rsol}}^2)$, and m is an integer ($m \geq 0$). The frequency and feedback level can be independently obtained from (13) and (14). The onset oscillation frequency is able to be determined solely from (13) once the delay τ is fixed and the feedback level is determined from (14).

Both the numerical and analytic results of the normalized frequency $\Omega/(2\pi f_{\text{rsol}})$ as a function of the delay ratio τf_{rsol} are shown in Fig. 1(a). The solid curve is from (13) and matches well with those from (11) and (12). The curve with open circles is derived from numerical calculations. Several possible solutions actually arise, e.g., branches A, B, and C in Fig. 1(a) at a fixed ratio. Each branch has its own origin. For comparison, the unperturbed cavity modes are also plotted as marked with boxes. With a detailed examination, for a delay ratio less than one, branch A obviously corresponds to the relaxation oscillation, branch B corresponds to the fundamental cavity mode, and branch C corresponds to the second cavity mode. The second cavity mode actually has little effect on the relaxation oscillation and the system can be viewed as a two-resonator coupled system. The respective oscillation frequency has been pushed away from the unperturbed one, just like the weakly coupled situation. At the critical point with the delay ratio τf_{rsol} equal to the integer $n(n = 1)$, the system behaves as a coupled cavity with two identical resonance frequencies. In such a situation the resonance frequencies are shifted the farthest. A slight increase of the delay ratio swaps the roles of the branches. This implies that the roles of branch A and branch B interchange for a delay ratio between one and two. Branch B is now for the relaxation oscillation and branch A is the first external-cavity mode. This behavior repeats with branch B replaced by branch C for the delay ratio between two and three, as indicated in [29]. Branch C is the relaxation oscillation and branch B is the second external-cavity mode. The decision of the true branch depends on the lowest level R_{ext} required. The threshold R_{ext} for different branches can be obtained by substituting the corresponding Ω's and τ such as points a, b, and c in the Fig. 1(a) into (14). In the typical case of the delay ratio $\tau f_{\text{rsol}} = 3/2$ (i.e., $L_{\text{ext}} = 7.92$ cm) and $I = 1.3I_{\text{th}}$, three possible oscillation angular frequencies with respect to branches B, A, C are at $\Omega = 2\pi_{\text{rsol}}$, $\Omega = (0.61) \times (2\pi f_{\text{rsol}})$, and $\Omega = (1.41) \times (2\pi f_{\text{rsol}})$, respectively, with the required threshold feedback levels of R_{ext} at 6.64×10^{-6} (-51.77 dB), 1.946×10^{-4} (-37.1 dB), and 3.64×10^{-2} (-14.38 dB), respectively. It turns out that the oscillation frequency of the first intensity fluctuation comes from branch B, which originates from the relaxation oscillation. Alternatively, for a short delay such as $\tau f_{\text{rsol}} = 0.568$ (i.e., $L_{\text{ext}} = 3$ cm), the predicted frequences are at 2.7 GHz from branch A and 5.28 GHz from branch B with $R_{\text{ext}} = 5.67 \times 10^{-6}$ (-52.46 dB) and $R_{\text{ext}} = 3.55 \times 10^{-2}$ (-14.49 dB), respectively. Obviously, the first oscillation comes from branch A and is also from the relaxation oscillation. The big difference in the threshold for the second instability recalls the features of the small-signal gain roll-off of 12 dB/octave for the frequency above f_{rsol}.

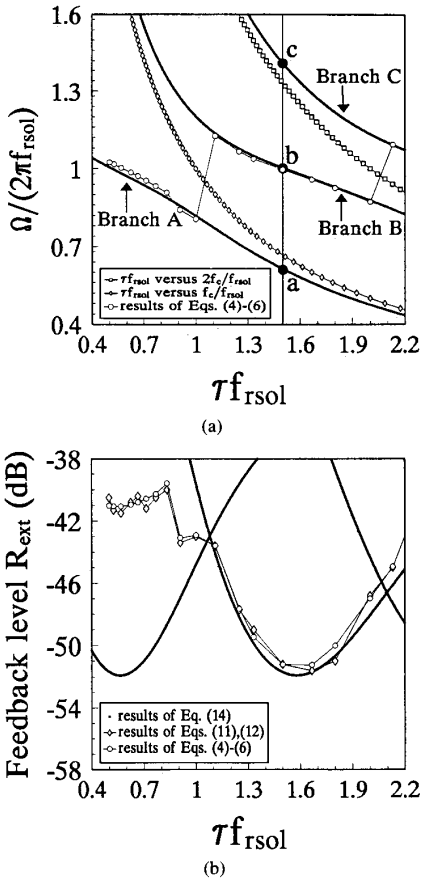

Fig. 1. (a) The normalized angular frequencies $\Omega/(2\pi f_{\text{rsol}})$ of the onset oscillation frequency and (b) the threshold feedback levels R_{ext} versus the delay ratio τf_{rsol} for $I = 1.3I_{\text{th}}$ and $\epsilon = 1.76 \times 10^{-23}$ m^3.

The threshold feedback level for the first oscillation, predicted from both (11) and (12) and from (13) and (14) is illustrated in Fig. 1(b) as a function of delay ratio. It reveals that the predictions with a delay ratio larger than one sufficiently correlates to the numerical computations in the next section. Whereas, for the delay ratio $\tau f_{\text{rsol}} < 1$, the results from (13) and (14) cannot match well with the numerical results. This implies that (13) and (14) are oversimplified for short delays. The deviation from (14) is

about 11 dB and only about 1 dB from (11) and (12). The frequency deviation from (13) is about 6 percent and about 3 percent from (11) and (12). Despite this oversimplification, the simple expressions of (13) and (14) are still capable of easily predicting the onset oscillation frequency and threshold feedback level, especially in the long delay cases.

III. Numerical Results

The transitions to chaos of the limit-cycle solutions depend essentially on the subsequent instabilities. The QP route may occur as the second frequency is also from the Hopf bifurcation with a frequency incommensurate to the first. Additionally, the successive subharmonic-oscillation route may occur as the second frequency is rational with respect to the first. The PD route may arise as the successive half subharmonic components emerge in the spectrum. In principle, the second instability should be analyzed around the limit-cycle solution [30]. Such an analysis needs the detailed information about the solution of the limit cycle, which in turn, is derived from numerical computation. Hence, the instability sequences and routes to chaos are further confirmed via numerical computation with the fourth-order Runge–Kutta algorithm. The calculations begin without optical feedback within the first round-trip period τ. In avoiding the errors from the transient states, the first 15 000 round-trip periods are dropped out and calculations are put in action for another 4096 round-trip periods. The frequency spectra of the output photon density are obtained by the FFT program with a resolution below 1 MHz after 64-fold ensemble averaging for the sake of improving the accuracy. The possibility of the periodic-doubling route is tested by choosing the delay ratio to be within the region of $1/2$ to 2. The relaxation oscillation frequency f_{rsol} of the solitary laser is about equal to 2.84 GHz with the bias current $I = 1.3I_{\text{th}}$. The condition of $\omega_0\tau = -\arctan(\alpha)$ for the minimum linewidth is applied during the calculations [6], [25], [31–[33]. The dynamic transitions are distinguished from the variations of the qualitative behaviors of the power spectra.

A. The First Hopf Bifurcation

For completeness, the dependency of the first oscillation on the damping factor η are checked by changing the gain saturation factor ϵ, which originates from spatial hole burning and partially contributes toward the damping factor η in (8). The $H_{\max}$ becomes 17.32 and η becomes 0.0289 for $\epsilon = 0$. The onset oscillation frequency and threshold feedback level as a function of the delay ratio are shown in Fig. 2(a) and (b), respectively. The first oscillation frequency still occurs around the relaxation oscillation frequency, but with a smaller shifting range. The threshold feedback level is less than that without the gain saturation effect. Thus, semiconductor lasers with a small gain saturation factor are more susceptible to optical feedback. It is believed that the first instability from the relaxation oscillation is always attributed to the inherent properties of the high-peak $H_{\max}$ and low-damping factor η of semiconductor lasers.

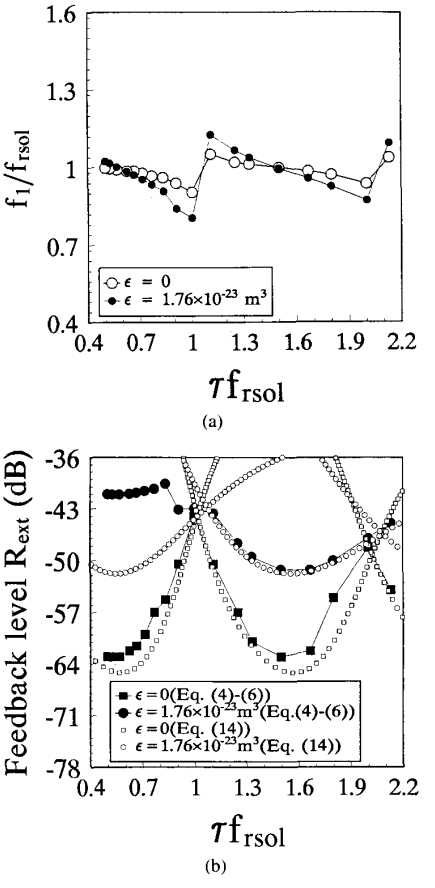

Fig. 2. The numerical results of (a) the normalized first oscillation frequencies f_1/f_{rsol} and (b) the threshold feedback levels R_{ext} versus the delay ratio τf_{rsol} for $\epsilon = 1.76 \times 10^{-23}$ m^3 and $\epsilon = 0$.

B. Routes to Chaos

The second instability emerges as the feedback strength is further increased. The different routes are differentiated with a variation of the delay ratio.

1) Quasi-Periodic Route: According to our observations, this route often occurs as the delay ratio is set above 0.9. The scenario is that the stationary dc solution bifurcates first into a stable limiting cycle and further into a torus, followed either by an intermediate frequency-locking solution or directly by a chaotic state without any frequency locking, similar to those in [14]. The typical transitions in terms of the power spectra of the photon density are illustrated in Fig. 3 in the case of $L_{\text{ext}} = 7.92$ cm (i.e., $f_c = 1/\tau = 1.89$ GHz) with τf_{rsol} equal to $3/2$. The calculated first onset frequency $f_1 = 2.8$ GHz is very close to f_{rsol}, as predicted in the previous section. The second oscillation frequency $f_2 = 2.15$ GHz is higher than, but near, the fundamental cavity frequency f_c. This reveals that the second oscillation may originate from the funda-

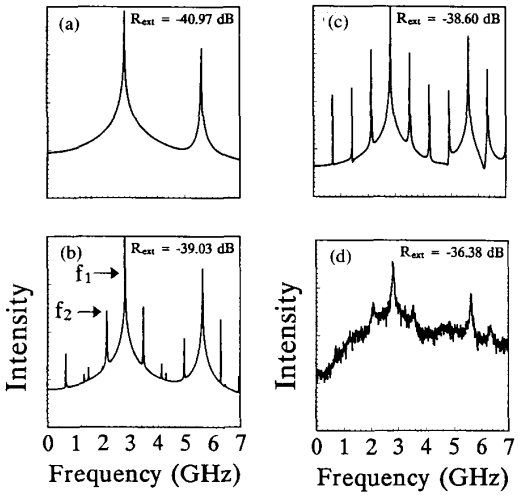

Fig. 3. The power spectra of photon density for the quasi-periodic route interrupted by the interlocking state at $f_1/f_2 = 4/3$ with $L_{ext} = 7.92$ cm and (a)$R_{ext} = -40.97$ dB, (b) $R_{ext} = -39.03$ dB, (c) $R_{ext} = -38.60$ dB, and (d) $R_{ext} = -36.38$ dB.

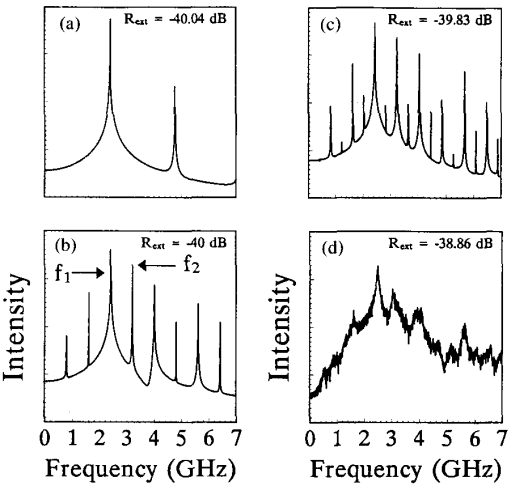

Fig. 4. The power spectra of photon density for the subharmonic cascade route with $L_{ext} = 4.8$ cm and (a) $R_{ext} = -40.04$ dB, (b) $R_{ext} = -40$ dB, (c) $R_{ext} = -39.83$ dB, and (d) $R_{ext} = -38.86$ dB.

mental-cavity mode in the observed case. These two basic frequencies f_1 and f_2 adjust themselves due to the nonlinear coupling to lock each other at $f_1/f_2 = 4/3$ and then become chaotic as the feedback strength is varied, as in Fig. 3 (c) and (d). Though the origin of the third oscillation frequency, which is a necessary ingredient of chaos, is not identified here. The third frequency is believed to have something to do with the second cavity mode. The details will be discussed elsewhere.

2) Subharmonic-Oscillation Route: These phenomena are observed with the delay ratio around the region of 0.8–0.9. The typical power spectra of the photon density are demonstrated in Fig. 4 with $L_{ext} = 4.8$ cm (i.e., $f_c = 3.125$ GHz). The sequence of transitions in terms of the power spectra undergoes $f_1, f_1/3, f_1/6, \cdots$, to chaos, where f_1 is from the first Hopf bifurcation. The second frequency f_2 due to the second Hopf bifurcation is actually locked to $4f_1/3$ with $f_1 = 2.4$ GHz and $f_2 = 3.2$ GHz such that the outcome has an $f_1/3$ beaten component. The feedback thresholds of the first and second instabilities are at $R_{ext} = 5 \times 10^{-5}$ (-43.01 dB) and $R_{ext} = 1 \times 10^{-4}$ (-40 dB), respectively. According to our observations, there exist many fine interlocking structures (not shown here) so that the second oscillation is able to easily lock to the first one. Basically, the transition is similar to that in case 1.

3) Periodic-Doubling Route: The periodic-doubling route can be found with a delay ratio less than 0.8. The typical power spectra of the photon density for the situation of $L_{ext} = 3$ cm (i.e., $f_c = 1/\tau = 5$ GHz) are displayed in Fig. 5. The first Hopf bifurcation with frequency f_1 still near f_{rsol} occurs as the feedback is increased to a certain level. As the feedback level is further increased, the frequency spectra of the photon density reveal the components of $1/2, 1/4, 1/8, \cdots$, of f_1. The second instability is periodic

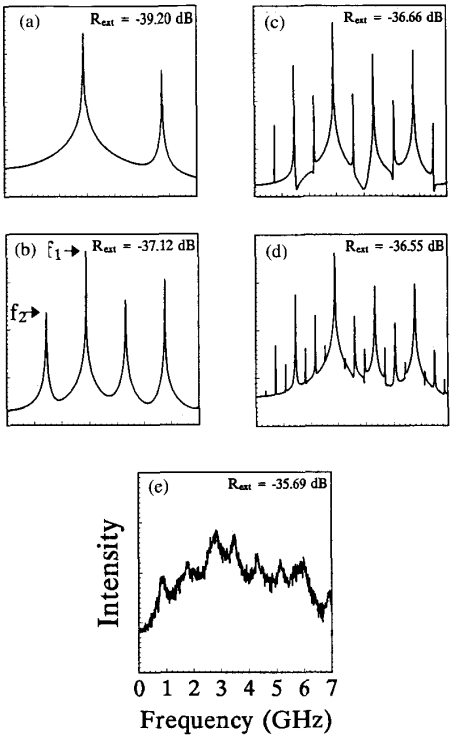

Fig. 5. The power spectra of photon density for the periodic-doubling route to chaos with $L_{ext} = 3$ cm and (a) $R_{ext} = -39.20$ dB, (b) $R_{ext} = -37.12$ dB, (c) $R_{ext} = -36.66$ dB, (d) $R_{ext} = -36.55$ dB, and (e) $R_{ext} = -35.69$ dB.

doubling rather than a Hopf bifurcation. It seems that the feedback effect on the optical intensity fluctuation becomes weakened and the second instability arises from the intrinsic nonlinearity of the laser diode itself under this very short delay case. The calculated frequencies f_1

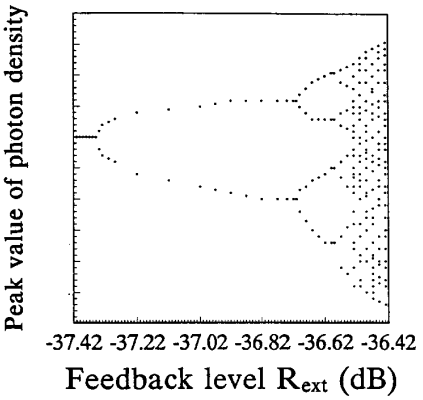

Fig. 6. The bifurcation diagram with peak values of the photon density as a function R_{ext} for $L_{ext} = 3$ cm.

and $f_1/2$ are at 2.85 and 1.425 GHz with $R_{ext} = 7.8 \times 10^{-5}$ (−41.07 dB) and $R_{ext} = 1.84 \times 10^{-4}$ (−37.35 dB), respectively. The bifurcation diagram, which is obtained by taking the local maxima of the photon density fluctuations as a function of R_{ext}, is illustrated in Fig. 6 with the characteristic scaling constant being about equal to 4.833, which is close to the universal constant predicted by Feigenbaum [18].

IV. Conclusions

The intensity fluctuations and the related routes to chaos in semiconductor lasers with short delay feedback have been extensively investigated in this paper. The conditions of the quasi-periodic, and periodic-doubling routes occurring in terms of the delay ratio are indicated. The periodic-doubling route dominates the transitions to chaos in the short external cavity for delay ratios smaller than 0.8. The quasi-periodic scenario is mostly observed for delay ratios above 0.9. The subharmonic cascade is favorable for delay ratios around the intermediate region of 0.8 to 0.9. During the transitions, the first oscillation apparently takes place from the relaxation oscillation for typical semiconductor lasers with a low damping factor ($\eta \simeq 0.1$). The second instability may be either from the fundamental-cavity mode with a delay ratio around unity or from another nonlinearity in the very short delay case and deserves further study.

Acknowledgment

The authors wish to thank the reviewers for their comments and suggestions. The quotation in the introduction about the occurrence of intermittency near threshold and strong feedback in [16] was suggested by a reviewer. The comments on (11) and (12) and Fig. 1 by another reviewer are also warmly appreciated.

References

[1] L. Goldberg, H. F. Taylor, A Dandridge, J. F. Weller, and R. O. Miles, "Spectral characteristics of semiconductor lasers with optical feedback," *IEEE J. Quantum Electron.*,, vol. QE-18, pp. 555–564, Apr. 1982.

[2] F. Favre, D. LeGuen, and J. C. Simon, "Optical feedback effects upon laser diode oscillation field spectrum," *IEEE J. Quantum Electron.*, vol. QE-18, pp. 1712–1717, Oct. 1982.

[3] R. Wyatt and W. J. Devlin, "10 kHz linewidth 1.5 μm InGaAsP external cavity laser with 55 nm tuning range," *Electron. Lett.*, vol. 19, pp. 110–112, Feb. 1983.

[4] D. Lenstra, B. H. Verbeek, and A. J. den Boef, "Coherence collapse in single-mode semiconductor lasers due to optical feedback," *IEEE J. Quantum Electron.*, vol. QE-21, pp. 674–679, June 1985.

[5] T. Mukai and K. Otsuka, "New route to optical chaos: Successive-subharmonic-oscillation cascade in a semiconductor laser coupled to an external cavity," *Phys. Rev. Lett.*, vol. 55, pp. 1711–1714, Oct. 1985.

[6] R. W. Tkach and A. R. Chraplyvy, "Regimes of feedback effects in 1.5 μm distributed feedback lasers," *J. Lightwave Technol.*, vol LT-4, pp. 1655–1661, Nov. 1986.

[7] Y. Cho and T. Umeda, "Observation of chaos in a semiconductor laser with delayed feedback" *Opt. Commun.*, vol. 59, pp. 131–136, Aug. 1986.

[8] H. Olesen, J. H. Osmundsen, and B. Tromborg, "Nonlinear dynamics and spectral behavior for an external cavity laser," *IEEE J. Quantum Electron.*, vol. QE-22, pp. 762–773, June 1986.

[9] J. Mϕrk, B. Tromborg, and P. L. Christiansen, "Bistability and low-frequency fluctuations in semiconductor laser with optical feedback: A theoretical analysis," *IEEE J. Quantum Electron.*, vol. 24, pp. 123–133, Feb. 1988.

[10] G. C. Dente, P. S. Durkin, K. A. Wilson, and C. E. Moeller, "Chaos in the coherence collapse of semiconductor lasers," *IEEE J. Quantum Electron.*, vol. 24, pp. 2441–2447, Dec. 1988.

[11] B. Tromborg and J. Mϕrk, "Nonlinear injection locking dynamics and the onset of coherence collapse in external cavity lasers," *IEEE J. Quantum Electron.*, vol. 26, pp. 642–654, Apr. 1990.

[12] J. Mϕrk, J. Mark, and B. Tromborg, "Route to chaos and competition between relaxation oscillations for a semiconductor laser with optical feedback," *Phys Rev. Lett.*, vol 65, pp. 1999–2002, Oct. 1990.

[13] B. Tromborg, and J. Mϕrk, "Stability analysis and the route to chaos for laser diodes with optical feedback" *IEEE Phonton. Technol. Lett.*, vol. 2, pp. 549–552, Aug. 1990.

[14] J. Mϕrk, B. Tromborg, and J. Mark, "Chaos in semiconductor lasers with optical feedback: Theory and experiment," *IEEE J. Quantum Electron.*, vol. 28, pp. 93–108, Jan. 1992.

[15] J. Sacher, W. Elsässer, and E. O. Göbel, "Intermittency in the coherence collapse of a semiconductor laser with external feedback," *Phys. Rev. Lett.*, vol. 63, pp. 2224–2227, Nov. 1989.

[16] J. Sacher, D. Baums, P. Panknin, W. Elsässer, and E. O. Göbel, "Intensity instabilities of semiconductor lasers under current modulation, external light injection, and delayed feedback," *Phys. Rev. A*, vol. 45, pp. 1893–1905, Feb. 1992.

[17] A. Ritter and H. Haug, "Theory of laser diodes with weak optical feedback. II. Limit-cycle behavior, quasi-periodic, frequency locking, and route to chaos," *J. Opt. Soc. Amer.* B, vol. 10, pp. 145–154, Jan. 1993.

[18] J. Ye, H. Li, and J. G. McInerney, "Period-doubling route to chaos in a semiconductor laser with weak optical feedback," *Phys. Rev. A*, vol. 47, pp. 2249–2252, Mar. 1993.

[19] R. Lang and K. Kobayashi, "External optical feedback effects on semiconductor injection laser properties," *IEEE J. Quantum Electron.*, vol. QE-16, pp. 347–335, Mar. 1980.

[20] N. Schunk and K. Petermann, "Stability analysis for laser diodes with short external cavities," *IEEE Phonton. Technol. Lett.*, vol. 1, pp. 49–51, Mar. 1989.

[21] K. Kikuchi and T. Lee, "Spectral stability analysis of weakly coupled external-cavity semiconductor lasers," *J. Lightwave Technol.*, vol. LT-5, pp. 1269–1272, Sept. 1987.

[22] J. P. van der Ziel, "Modelocking of semiconductor lasers," in *Semiconductors and Semimetals*, vol. 22B, W. T. Tsang, Ed. Orlando, FL: Academic, 1985, pp. 1–68.

[23] K. Y. Lau, "Short-pulse and high frequency signal generation in semiconductor lasers," *J. Lightwave Technol.*, vol. 7, pp. 400–419, 1989.

[24] A. G. Weber, M. Schell, G. Fischbeck, and D. Bimberg, "Generation of single femtosecond pulse by hybrid mode locking of a semiconductor laser," *IEEE J. Quantum Electron.*, vol. 28, pp. 2220–2229, Oct. 1992.

[25] N. Schunk and K. Petermann, "Numerical analysis of the feedback regimes for a single-mode semiconductor laser with external feedback," *IEEE J. Quantum Electron.*, vol. 24, pp. 1242–1247, July 1988.
[26] G. P. Agrawal and N. K. Dutta, *Long-Wavelength Semiconductor Lasers*. New York: Van Nostrand Reinhold, 1986, ch. 6.
[27] K. Petermann, *Laser Diode Modulation and Noise*. Dordrecht, The Netherlands: Kluwer Academic, 1988.
[28] B. Tromborg, J. H. Osmundsen, and H. Olesen, "Stability analysis for a semiconductor laser in an external cavity," *IEEE J. Quantum Electron.*, vol. QE-20, pp. 1023–1032, Sept. 1984.
[29] J. S. Cohen, R. R. Drenten, and B. H. Verbeek, "The effect of optical feedback on the relaxation oscillation in semiconductor lasers," *IEEE J. Quantum Electron.*, vol. 24, pp. 1989–1995, Oct. 1988.
[30] A. Ritter and H. Haug, "Theory of the bistable limit cycle behavior of laser diodes induced by weak optical feedback," *IEEE J. Quantum Electron.*, vol. 29, pp. 1064–1070, Apr. 1993.
[31] J. Mørk, M. Semkow, and B. Tromborg, "Measurement and theory of mode hopping in external cavity lasers," *Electron. Lett.*, vol. 26, pp. 609–610, Apr. 1990.
[32] J. O. Binder and G. D. Cormack, "Mode selection and stability of a semiconductor laser with weak optical feedback," *IEEE J. Quantum Electron.*, vol. 25, pp. 2255–2259, Nov. 1989.
[33] J. Mørk and B. Tromborg, "The mechanism of mode selection for an external cavity laser," *IEEE Photon. Technol. Lett.*, vol. 2, pp. 21–23, Jan. 1990.

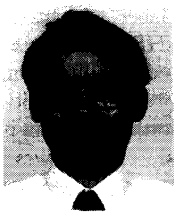

Yao Huang Kao, (M'86) was born in Tainan, Taiwan, Republic of China in 1953. He received the B.S., M.S., and Ph.D. degrees from National Chiao-Tung University in electronic engineering in 1975, 1977, and 1986, respectively. Since 1986, he has joined the faculty of the department of communication engineering, National Chiao-Tung University, and now becomes a full professor. He has also been a visiting scholar, working in nonlinear circuit, in University of California, Berkeley in 1988. His current research interests involve nonlinear dynamics and chaos, high speed optical communications, and microwave circuit designs.

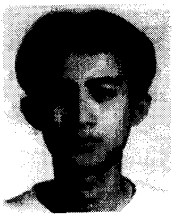

Nien Ming Wang, was born in Taiwan, Republic of China, in 1969. He received the B.S. degree in electrical engineering from National Cheng-Kung University and the M.S. degree in communication engineering from Chiao-Tung University, in 1991 and 1993, respectively. His research interests are stability and modulation properties of laser diode under high speed operations.

Hong Ming Chen, was born in Pingtung, Taiwan, Republic of China, in 1962. He received the B.S. degree in physics from Fu-Jen Catholic University and the M.S. degree in electro-optical engineering from Chiao-Tung University, in 1986 and 1992, respectively. Since 1992, he has joined the Opto-Electronics & Systems Laboratories of Industrial Technology Research Institute, Hsinchu, Taiwan. He is currently working on optical waveguide devices on silicon.